Available online at www.sciencedirect.com
SCIENCE DIRECT®
Catalysis Today 98 (2004) 583–587
CATALYSIS TODAY
www.elsevier.com/locate/cattod

Partial oxidation of methane to syngas over $BaTi_{1-x}Ni_xO_3$ catalysts

Cuili Guo, Jinli Zhang, Wei Li*, Pingfan Zhang, Yiping Wang

Key Laboratory of Green Chemical Technology, School of Chemical Engineering and Technology, Tianjin University, Tianjin 300072, China

Abstract

Performances of $BaTi_{1-x}Ni_xO_3$ perovskites, prepared using sol–gel method, as catalysts for partial oxidation of methane to syngas have been studied. The catalysts were characterized by XRD, BET and TEM. The experimental studies showed the calcination temperature and Ni content exhibited a significant influence on catalytic activity. Among catalysts tested, the catalyst $BaTi_{0.8}Ni_{0.2}O_3$ exhibited the best activity and excellent stability.

Keywords: Partial oxidation; Methane; Syngas; Perovskite; Catalyst

1. Introduction

Partial oxidation of methane (POM) to syngas has recently attained a lot of attentions. Compared with the conventional steam reforming that is highly energy and capital intensive, POM is more energy efficient and can be carried out at lower investment and will produce synthesis gas with a H_2/CO ratio of ca. 2, which is suitable for syntheses of methanol and hydrocarbons.

Many catalysts have been reported to be active and selective towards POM to synthesis gas. Noble metal catalysts, like Ir, Pt, Pd, Rh and Ru, particularly Ru catalysts [1–4], have been found to exhibit high activity with good long-term stability. However, because of their high cost and limited availability of noble metals, it is more practical to develop alternative catalysts. The Ni catalyst, usually supported on alumina and silica, is the most extensively studied one as such an alternative [5–11]. However, Ni catalysts suffer from the problem of coke formation. To prevent the carbon deposition over Ni catalysts, various additives have been applied [12–16]. High dispersion of metal species over catalyst or the use of alkali or alkaline earth metal oxides in catalyst may reduce coke formation. Hayakawa et al. [15] have prepared $Ca_{0.8}Sr_{0.2}Ti_{0.8}Ni_{0.2}$ catalyst for POM. This catalyst showed high activity for synthesis gas production. XRD studies on the spent catalysts indicated that nickel oxide segregated from the perovskite structure and was reduced to nickel metal particles that were thought to be the active catalytic species. Lago et al. [17] observed that a series of $LnCoO_3$ (Ln = La, Pr, Nd, Sm, and Gd) perovskites presented high activity and selectivity for POM to synthesis gas. Choudhary et al. [18] reported that complex oxides with a perovskite structure, like $LaNiO_3$, $La_{0.8}Ca$(or Sr)$_{0.2}NiO_3$ and $LaNi_{1-x}Co_xO_3$ (x = 0.2–1.0), were resistant to coking. Takehira et al. [19] found that Ni supported on perovskites, prepared by solid phase crystallization, like $Ni_{0.2}/ATiO_3$ (A: Ca, Sr or Ba), showed high activity and selectivity as well as very low coke formation. They explained that the good catalyst performance was obtained from highly dispersed and stabilized Ni metal particles on perovskites. These studies suggest that high dispersion of metal species and/or the use of alkaline earth metals are beneficial to improve the catalytic performance for POM.

In this work, POM was investigated over novel $BaTi_{1-x}Ni_xO_3$ perovskite catalysts prepared by sol–gel method. Especially, the effect of Ni loading and calcination temperature will be discussed.

* Corresponding author. Tel.: +86 22 274 01999.
E-mail address: liwei@tju.edu.cn (W. Li).

0920-5861/$ – see front matter © 2004 Elsevier B.V. All rights reserved.
doi:10.1016/j.cattod.2004.09.012

2. Experimental

2.1. Catalyst preparation

$BaTi_{1-x}Ni_xO_3$ perovskite catalysts were prepared by using the sol–gel method with x values varying from 0 to 0.3. To prepare the catalyst, tetrabutyl titanate, citric acid and glycol were mixed and stirred to form a solution under reflux. Then $Ba(NO_3)_2$ and $Ni(NO_3)_2{\cdot}6H_2O$ were added into the solution with stirring and the nitrates were decomposed. A gel was obtained by adding triethylamine into the solution. The gel was then dried at 350 °C for 3 h and the dried gel was calcined at 600, 700 and 800 °C, respectively, for another 3 h to obtain three different catalysts.

2.2. Characterization of the catalysts

The catalyst characterization was conducted by using XRD, TEM and BET. The powder X-ray diffraction (XRD) patterns of the catalysts were obtained by using a Rigaku 2038 diffractometer with a Cu Kα radiation at a rate of 4 °/min. The particle textures of the catalysts were investigated by using a JEOL TEM-100X II transmission electron microscope. The specific surface areas of the catalysts were calculated from N_2 adsorption isotherms that were determined with a Chem BET-3000 system.

2.3. Measurement of catalytic activity

The catalyst was pressed into pellets that were further crushed into particles of 40–60 mesh. POM was carried out in a fixed bed quartz reactor (8 mm i.d.) at atmospheric pressure. A 300 mg of catalyst was loaded. The feed gas mixture was composed of CH_4, O_2 and He with space velocity from 2.1×10^4 to 8.6×10^4 ml h^{-1} g^{-1}. The reactor was kept in a tubular furnace and its temperature was controlled by a thermocouple, which was placed in the center of the catalyst bed. The products were analyzed on-line by a SP3420 gas chromatograph equipped with a TCD detector using a TDX-01 column.

3. Results and discussion

3.1. The characters of $BaTi_{1-x}Ni_xO_3$ catalysts

X-ray diffraction patterns of $BaTiO_3$ powders after calcination are shown in Fig. 1. In this figure, the catalysts calcined at 600 and 700 °C exhibit an intensive peak of $BaTiO_3$ and a weak peak of $BaCO_3$. The catalyst calcined at 800 °C shows an almost uniform perovskite phase, while the peak of $BaCO_3$ disappears. These results indicate that the calcination temperature has a significant effect on the formed perovskite phase.

XRD patterns of $BaTi_{1-x}Ni_xO_3$ catalysts calcined at 700 °C are presented in Fig. 2. For the catalyst with a low content of Ni, like $BaTi_{0.9}Ni_{0.1}O_3$, perovskite is the dominant phase and a small amount of $BaCO_3$ is observed, indicating that nickel species were homogeneously incorporated in the perovskite structure. For the catalyst with a higher loading of Ni like $BaTi_{0.7}Ni_{0.3}O_3$, in addition to perovskite and $BaCO_3$, a small amount of NiO phase was also observed, which shows that nickel species were partly incorporated in the perovskite structure by replacing the Ti site and partly separated as NiO from the structure after the calcination of the precursors.

The crystal sizes of the samples based on the half-width of a diffraction peak using Scherrer formula and specific surface area of the samples are listed in Table 1. As seen in Table 1, the particle size increases and specific surface area

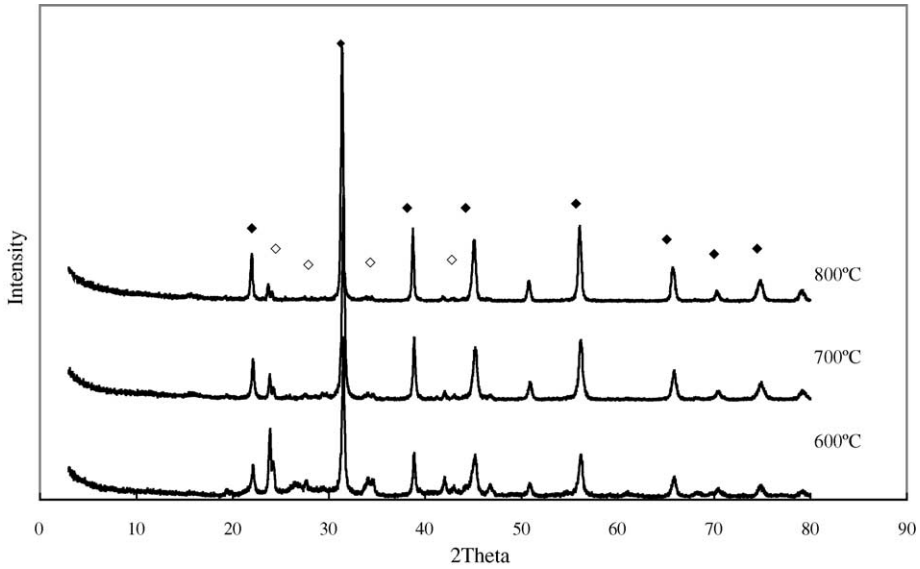

Fig. 1. XRD patterns of $BaTiO_3$ calcined at different temperatures: (◆) $BaTiO_3$; (◇) $BaCO_3$.

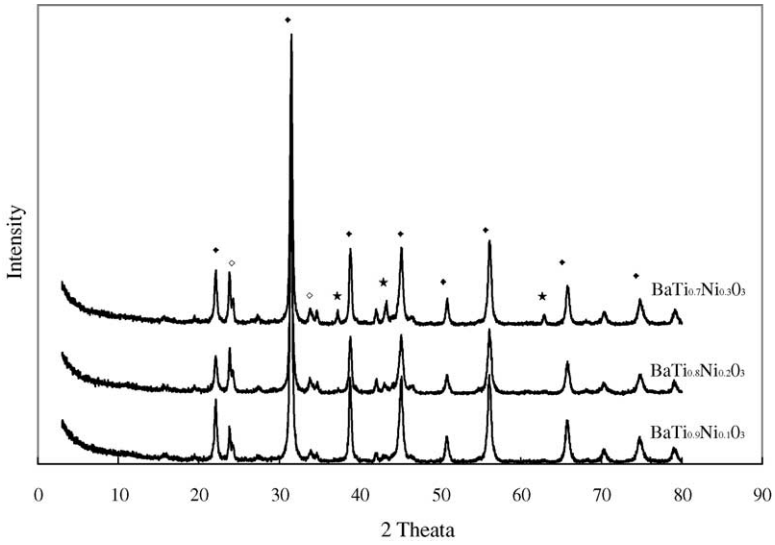

Fig. 2. XRD patterns of $BaTi_{1-x}Ni_xO_3$ calcined at 700 °C: (◆) $BaTiO_3$; (◇) $BaCO_3$; (★) NiO.

decreases with increasing calcination temperature, which indicate that the textural properties are significantly dependent on the calcination temperature.

3.2. POM over $BaTi_{1-x}Ni_xO_3$

Fig. 3 shows the catalytic activity for POM with a CH_4/O_2 feed molar ratio of 2:1 at a space velocity of 4.2×10^4 ml h^{-1} g^{-1} over $BaTi_{0.8}Ni_{0.2}O_3$ calcined at different temperatures. It is shown that the activation temperature of $BaTi_{0.8}Ni_{0.2}O_3$ increased with the increase in calcination temperature. The activity of $BaTi_{0.8}Ni_{0.2}O_3$ calcined at 800 °C was clearly lower than those calcined at 600 and 700 °C, which suggests that the calcination temperature influences the crystal size and concentration of crystal lattice oxygen in $BaTi_{0.8}Ni_{0.2}O_3$ catalysts.

The activities of catalysts calcined at 600 °C with different Ni loading were investigated at a CH_4/O_2 molar ratio of 2:1 and a space velocity of 4.2×10^4 ml h^{-1} g^{-1}. Fig. 4 shows the results over $BaTi_{1-x}Ni_xO_3$ catalysts with different Ni content. $BaTiO_3$ exhibited the lowest activity, even within the higher reaction temperature region. The activities of $BaTi_{1-x}Ni_xO_3$ (x = 0.1–0.3) increased significantly with the addition of Ni into the perovskite structure. Especially, when x was equal to 0.2, $BaTi_{0.8}Ni_{0.2}O_3$ exhibited the highest catalytic activity with a CH_4 conversion of 95% and a CO selectivity of 98%. When the content of Ni was too high (x = 0.3), it appears that the activity of $BaTi_{0.7}Ni_{0.3}O_3$ becomes lower than those of $BaTi_{0.8}Ni_{0.2}O_3$ and $BaTi_{0.9}Ni_{0.1}O_3$. These results suggest that doping Ni in the perovskite $BaTiO_3$ can increase the active species for the synthesis gas formation. The catalysts with higher content of Ni contain a small amount of NiO apart from the perovskite phase that may cause the formation of large nickel metal aggregates that induces a decrease in active surface area.

Table 1
Crystal size and specific surface area of $BaTiO_3$ at different temperatures

Calcination temperature (°C)	Surface area (m^2 g^{-1})	Particle size (nm)
600	16.1	13.9
700	12.3	16.9
800	10.5	21.2

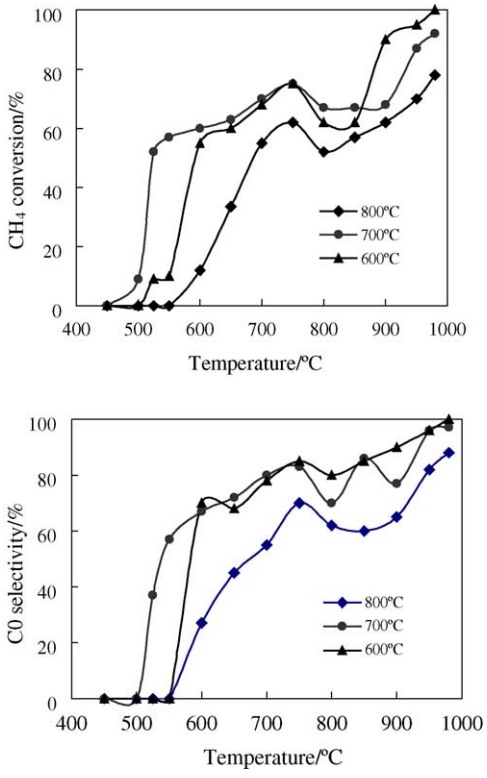

Fig. 3. CH_4 conversion or CO selectivity vs. temperature over $BaTi_{0.8}Ni_{0.2}O_3$ calcined at different temperatures.

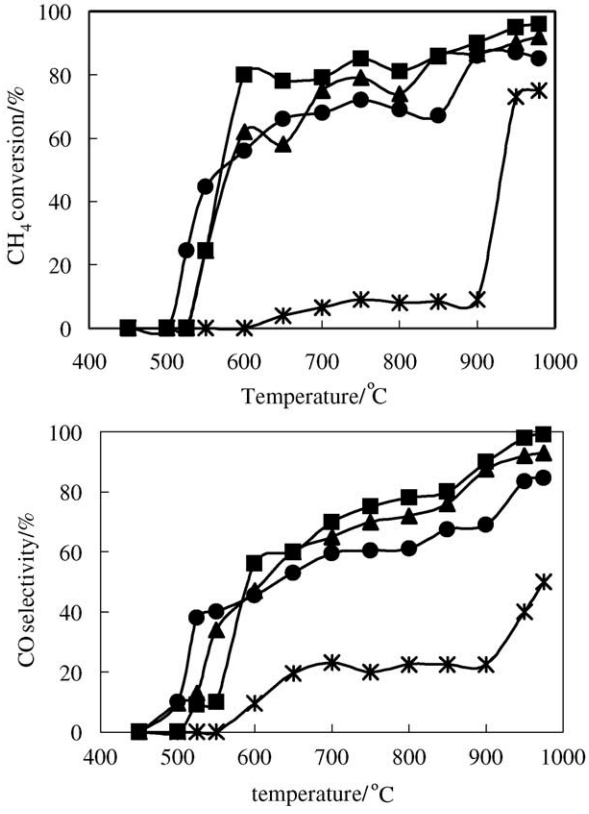

Fig. 4. Methane conversion or CO selectivity vs. temperatures over $BaTi_{1-x}Ni_xO_3$ with different nickel loading: (*) $BaTiO_3$; (▲) $BaTi_{0.9}Ni_{0.1}O_3$; (■) $BaTi_{0.8}Ni_{0.2}O_3$; (●) $BaTi_{0.7}Ni_{0.3}O_3$.

Fig. 4 also shows the influence of reaction temperature on the activity of $BaTi_{1-x}Ni_xO_3$ catalysts for POM to synthesis gas. The experimental results indicate that not only methane conversion but also CO selectivity increases with increasing reaction temperature. During the reactions, it was observed that the temperature of the catalyst bed of $BaTi_{1-x}Ni_xO_3$ was much higher than the furnace temperature when the reaction started, and then this temperature dropped to the same temperature as the furnace temperature. The significant temperature change in the catalyst bed reflects a cascade reaction mechanism in the investigated POM reactions, i.e., a complete oxidation of a part of methane into H_2O and CO_2 ($CH_4 + O_2 \rightarrow CO_2 + H_2O$) that is an exothermic reaction, followed by a CO_2 reforming and a steam reforming of the remaining methane ($CH_4 + CO_2 \rightarrow 2CO + 2H_2$ and $CH_4 + H_2O \rightarrow CO + 3H_2$), which are endothermic reactions. A transition from combustion to reforming was clearly seen in the product distributions of each reaction, i.e., CO_2 selectivity decreased and CO selectivity increased with increasing reaction temperature. The results are consistent with the results reported by Takehira et al. [19].

3.3. Effect of feed molar ratio

Table 2 lists the results of activity of $BaTi_{0.8}Ni_{0.2}O_3$ with different feed molar ratios of CH_4/O_2 for POM at 950 °C.

Table 2
Effect of CH_4/O_2 on the activity and the ratio of H_2/CO at 950 °C

CH_4/O_2 (mol/mol)	CH_4 conversion (%)	CO selectivity (%)	H_2/CO
1.0	93	90	1.8
1.9	94	93	1.9
2.0	95	98	2.0
2.1	91	99	2.0
2.4	79	98	2.1

The results show that for a 2.0 of CH_4/O_2 feed ratio, the catalyst presented a high activity with a methane conversion of 95% and a CO selectivity of 98%, respectively. The obtained H_2/CO of syngas was close to 2.

3.4. Effect of space velocity

Fig. 5 shows the effect of space velocity on catalytic activity of $BaTi_{1-x}Ni_xO_3$ at 950 °C with a CH_4/O_2 molar ratio of 2:1. The results exhibit that the methane conversion and CO selectivity significantly decreased with the increase in space velocity over $BaTi_{0.7}Ni_{0.3}O_3$ catalyst, while the activity of $BaTi_{0.95}Ni_{0.05}O_3$ and $BaTi_{0.8}Ni_{0.2}O_3$ slightly decreased with the increase in space velocity. These results seem to support the two-step reaction mechanism that the $BaTi_{1-x}Ni_xO_3$ catalyst might have promoted the reaction sequence of methane combustion to CO_2 and H_2O, and then the reforming of methane to syngas.

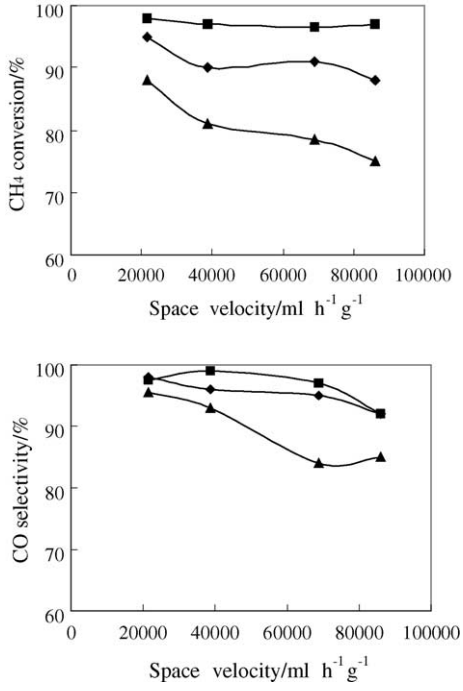

Fig. 5. Effect of the space velocity on CH_4 conversion and CO selectivity: (◆) $BaTi_{0.95}Ni_{0.05}O_3$; (■) $BaTi_{0.8}Ni_{0.2}O_3$; (▲) $BaTi_{0.7}Ni_{0.3}O_3$.

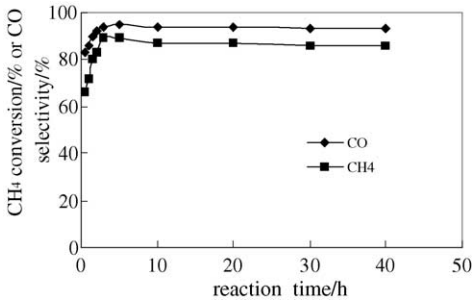

Fig. 6. Methane conversion and CO selectivity vs. reaction time.

3.5. Stability of $BaTi_{0.8}Ni_{0.2}O_3$ catalyst

Stability of $BaTi_{0.8}Ni_{0.2}O_3$ catalyst was also investigated. Fig. 6 presents the catalytic activity for POM versus reaction time at a CH_4/O_2 feed molar ratio of 2:1 and at 950 °C over $BaTi_{0.8}Ni_{0.2}O_3$ catalyst. Evidently, both CH_4 conversion and CO selectivity increase with the increasing reaction time during the initial 3 h reaction and thereafter remain almost unchanged during the 40 h life test, which suggests that the $BaTi_{0.8}Ni_{0.2}O_3$ catalyst is quite stable during high temperature reactions.

4. Conclusion

A series of $BaTi_{1-x}Ni_xO_3$ catalysts were prepared by the sol–gel method and were tested for the partial oxidation of methane to synthesis gas. Among the catalysts tested, the $BaTi_{0.8}Ni_{0.2}O_3$ catalyst exhibited the highest activity with excellent stability. The experimental investigations show that the partial oxidation of methane to syngas over $BaTi_{1-x}Ni_xO_3$ catalysts principally followed the two-step reaction mechanism via combustion and reforming reactions, i.e., part of the methane was first completely oxidized to H_2O and CO_2, and then the unconverted methane was reformed with CO_2 and H_2O to form syngas.

References

[1] E.P.J. Mallens, J.H.B.J. Hoebink, G.B. Marin, J. Catal. 167 (1997) 43.
[2] D. Wang, O. Dewaele, A.M.D. Groote, G.F. Froment, J. Catal. 159 (1996) 418.
[3] K.H. Hofstad, J.H.B.J. Hoebink, A. Holmen, G.B. Marin, Catal. Today 40 (1998) 157.
[4] M. Fathi, K.H. Hofstad, T. Sperle, O.A. Rokstad, A. Holmen, Catal. Today 42 (1998) 205.
[5] M.A. Goula, A.A. Lemonidou, W. Grunert, M. Baerns, Catal. Today 32 (1996) 149.
[6] V.A. Tsipouriari, Z. Zhang, X.E. Verykios, J. Catal. 179 (1998) 283.
[7] V.A. Tsipouriari, X.E. Verykios, J. Catal. 179 (1998) 292.
[8] R. Jin, Y. Chen, W. Li, W. Cui, Y. Ji, C. Yu, Y. Jiang, Appl. Catal. A 201 (2000) 71.
[9] A. Slagtern, H.M. Swaan, U. Olsbye, I.M. Dahl, C. Mirodatos, Catal. Today 46 (1998) 107.
[10] V.R. Choudhary, V.H. Rane, A.M. Rajput, Appl. Catal. 162 (1997) 235.
[11] V.R. Choudhary, B. Prabhakar, A.M. Rajput, J. Catal. 157 (1995) 752.
[12] H. Provendier, C. Petit, C. Estournes, S. Libs, A. Kiennemann, Appl. Catal. A 180 (1999) 163.
[13] W. Chu, W. Yang, L. Lin, Appl. Catal. A 235 (2002) 39.
[14] K. Takehira, T. Hayakawa, H. Harhara, A.G. Andersen, K. Suzuki, M. Shimizu, Catal. Today 24 (1995) 237.
[15] T. Hayakawa, H. Harihara, A.G. Andersen, K. Suzuki, H. Yasuda, T. Tsunoda, S. Hamakawa, A.P.E. York, Y.S. Yoon, M. Shimizu, K. Takehira, Appl. Catal. A 149 (1997) 391.
[16] T. Utaka, S.A. Al-Drees, J. Ueda, Y. Iwasa, T. Takeguchi, R. Kikuchi, K. Eguchi, Appl. Catal. A 247 (2003) 125.
[17] R. Lago, G. Bini, M.A. Pena, J.L.G. Fierro, J. Catal. 167 (1997) 198.
[18] V.R. Choudhary, B.S. Uphade, A.A. Belhekar, J. Catal. 163 (1996) 312.
[19] K. Takehira, T. Shishido, M. Kondo, J. Catal. 207 (2002) 307.